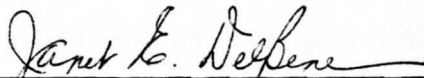



AN AB INITIO MOLECULAR ORBITAL
STUDY OF
PROTON AFFINITIES AND ION STRUCTURES

by
Sally Radovick

Submitted in Partial Fulfillment of the Requirements
for the Degree of
Master of Science
in the
Chemistry
Program



Advisor



Dean of the Graduate School

YOUNGSTOWN STATE UNIVERSITY

August, 1978

ABSTRACT

AN AB INITIO MOLECULAR ORBITAL
STUDY OF
PROTON AFFINITIES AND ION STRUCTURES

Sally Radovick

Master of Science

Youngstown State University, 1978

Ab initio SCF calculations have been performed in this study of the relative proton affinities of the carbonyl bases R_2CO and the hydroxyl bases ROH , and of the structures of the ions R_2COH^+ and ROH_2^+ , where R is one of the iso-electronic saturated groups CH_3 , NH_2 , OH , and F . For the bases R_2CO , the calculated order of proton affinity with respect to R is $NH_2 > CH_3 > OH > H > F$, which is the same order predicted for the monosubstituted carbonyl bases $RCHO$. A comparison of the proton affinities of corresponding mono- and disubstituted carbonyl bases indicates that replacement of the hydrogen atom in $RCHO$ by a second R group causes a further change in the proton affinity of the base in the same direction as observed upon substitution of the first R group, although the effect of two substituents is less than additive except in F_2CO . Protonation of carbonyl bases leads to an increase in the C-O bond distance and a decrease in the bond distance between the carbonyl carbon and the substituent, the magnitude of which depends on the substituent. Protonation also causes changes in the bond angles

about the carbonyl carbon which are essentially independent of the nature of the substituent, but strongly dependent on the position of the proton relative to the two substituents. Changes in bond lengths and bond angles and in the electron distribution upon protonation of bases R_2CO are similar to the changes which occur upon protonation of the bases $RCHO$.

For the bases ROH , the predicted order of proton affinity with respect to R is $CH_3 > H > NH_2 > OH > F$, which is dramatically different from the order of proton affinity of mono- and disubstituted carbonyl compounds. Oxygen protonation leads to an increase in the length of the bond between the oxygen and a first row atom. This increase is larger when the protonated oxygen is a carbonyl rather than a hydroxyl oxygen. As in the protonated carbonyls, the O-H distance in the protonated species ROH_2^+ is relatively constant, independent of the substituent. These protonated species also show only a relatively small variation in the H-O-H angle and in the angle between the O-X bond and the bisector in the H-O-H angle. The study of the electron redistribution upon protonation of bases ROH suggests that the mechanism by which stabilization occurs is quite different from that in the ions R_2COH^+ and $RCHOH^+$.

Two computational methods to simplify the computation of proton affinities have been evaluated. Studies of the rigid monomer restriction applied to ions R_2COH^+ indicate that this is a severe approximation since it neglects the

significant structural changes which occur in the relaxed ions, thereby altering the predicted order of proton affinity. The rigid monomer restriction is less severe structurally and energetically in ROH_2^+ than in R_2COH^+ and RCHOH^+ . Reasonable estimates of relative proton affinities without full geometry optimization at the 4-31G level can be obtained from calculations with the 4-31G basis set using optimized STO-3G geometries for bases and ions.

ACKNOWLEDGMENTS

I would like to extend my sincerest and deepest appreciation to my advisor Dr. Janet Del Bene under whose guidance I am proud to have studied. I am eternally grateful and indebted to her for the wealth of knowledge she imparted to me, as well as for her time, patience and understanding. Also, I would like to thank my family, for without their encouragement, sacrifices and belief in the value of education, and especially their love, I would not have made it this far in my education. To them I owe a debt that can never be repaid. Finally, I would like to acknowledge the assistance of the Youngstown State University Computer Center.

TABLE OF CONTENTS

	PAGE
ABSTRACT	ii
ACKNOWLEDGMENTS	v
TABLE OF CONTENTS	vi
LIST OF FIGURES	viii
LIST OF TABLES	ix
CHAPTER	
I. INTRODUCTION	1
Statement of the Problem	
Purposes of the Study	
II. METHOD OF CALCULATION	5
Determination of the SCF Ground State Wavefunction	5
Basis Sets	9
Geometry Optimization	12
Calculation of Proton Affinities	14
III. SUMMARY	15
Findings	15
Proton Affinities of R_2CO (STO-3G)	15
Structures of R_2COH^+ (STO-3G)	21
The Rigid Monomer Restriction in R_2COH^+ (STO-3G)	32
Proton Affinities of ROH (STO-3G)	35
Structures of ROH_2^+ (STO-3G)	39

The Rigid Monomer Restriction in ROH ₂ ⁺ (STO-3G)	45
Proton Affinities (4-31G)	47
Ion Structures (4-31G)	48
Methyl Substituent Effects on Proton Affinities	54
4-31G Proton Affinities from STO-3G Geometries	59
Conclusions	64
REFERENCES	68

LIST OF FIGURES

FIGURE	PAGE
1. Equilibrium Structures of R_2COH^+	25
2. Equilibrium Structures of ROH_2^+	42
3. Equilibrium Structure of $(CH_3)_2OH^+$	53

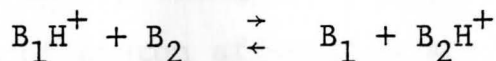
LIST OF TABLES

TABLE	PAGE
1. Relative Proton Affinities of Substituted Carbonyl Compounds (STO-3G)	16
2. Mulliken Population Data for R_2COH^+ (STO-3G)	19
3. Structures of Bases R_2CO and Ions R_2COH^+ (STO-3G)	22
4. Mulliken C-O and C-X Overlap Populations	26
5. The Effect of the Rigid Monomer Restriction on the Computed Relative Proton Affinities of R_2CO (STO-3G)	33
6. Relative Proton Affinities of Bases ROH (STO-3G)	36
7. Mulliken Population Data for Bases ROH and Ions ROH_2^+ (STO-3G)	38
8. Structures of Bases ROH and Ions ROH_2^+ (STO-3G)	40
9. Equilibrium Structures of Acetone, Carbonic Acid, Protonated Acetone, and Protonated Carbonic Acid (4-31G)	49
10. Equilibrium Structures of H_3O^+ , $CH_3OH_2^+$, and $(CH_3)_2OH^+$ and Their Bases (4-31G)	51
11. Equilibrium Structures of $(CH_3)_2O$ and $(CH_3)_2OH^+$ (STO-3G)	52
12. Relative Proton Affinities of H_2O , CH_3OH , and $(CH_3)_2O$ and H_2CO , CH_3CHO , and $(CH_3)_2CO$	55
13. Ionization Potentials of H_2O , CH_3OH , and $(CH_3)_2O$ and H_2CO , CH_3CHO , and $(CH_3)_2CO$	57
14. Relative Proton Affinities of Methyl Substituted Bases Determined From 4-31G Calculations	60
15. Relative Proton Affinities of Bases ROH	63

CHAPTER I

INTRODUCTION

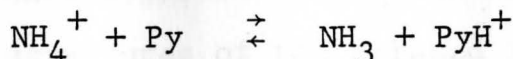
For many decades, organic chemists have studied the effects of substitution on the basicity of a molecule toward a proton in solution. From comparative observations, relationships such as the Hammett substituent constants have been derived, and explanations of the order of basicity or proton affinity have been espoused.¹ Recent advances in high pressure mass spectrometry and pulsed ion cyclotron resonance spectroscopy have made it possible to study the previously reported solution reactions in the gas phase by measuring the equilibrium constant K for the proton transfer reaction



and from K determining ΔG and ΔH values.²⁻⁶ A comparison

of the solution and the gas-phase results shows that the order of basicity or proton affinity may be different.

For example, for the proton transfer reaction involving NH_3 and pyridine (Py)



the ΔH values are -15.8 ,² $+4.7$,⁷ and $+7.7$ ⁷ kcal/mol in the gas phase, in HSO_3F , and in H_2O , respectively. Therefore the traditional arguments given to explain the order of basicity of molecules in solution were concerned not with

the intrinsic proton affinities of the bases but with the proton affinities of the bases as modified by the solvent. It is obvious that a critical rethinking of the explanation of the order of base strength is necessary.

Chronologically paralleling as well as complementing experimental gas phase data are ab initio molecular orbital calculations which are particularly suited for studying the proton affinities of bases in the gas phase.^{6,8-19} Calculations can provide a numerical basis for understanding the factors which influence the basicity of a molecule toward a proton. Brought to light by theoretical data are the previously inaccessible data regarding changes in bond lengths and bond angles as well as electron redistribution upon protonation. In addition to explaining the gas phase results, the theoretical data are also significant as a first step toward interpreting the solution phase data. Ab initio studies of proton affinities are therefore an area of intense interest at this time.

In this work the relative proton affinities of the bases R_2CO , where R is any one of the isoelectronic saturated groups CH_3 , NH_2 , OH and F have been computed, and substituent effects on the proton affinities have been evaluated. To this end, the structures of the relaxed ions R_2COH^+ have been determined, and comparisons have been made between the structures of the bases R_2CO and the structures of the corresponding ions R_2COH^+ . In addition, an analysis of substituent effects on the proton affinities of bases ROH

and the effect of protonation on the structures of ions ROH_2^+ has been made. The structures and energies of the bases ROH and the ions ROH_2^+ have been reported by Pople and coworkers²⁰ in a comprehensive study of systems with the general formula H_mABH_n , but no analysis of these data has been made with respect to the protonation process.

The purposes of the present study are:

- (1) to determine the relative proton affinities of the bases R_2CO and to analyze the effect of varying the R group on the proton affinity of these bases;
- (2) to evaluate the effect of mono- vs. disubstitution on the proton affinities of carbonyl bases;
- (3) to determine the equilibrium structures of the ions R_2COH^+ ;
- (4) to compare the structures of the ions R_2COH^+ with each other and with the corresponding ions RCHOH^+ ;
- (5) to analyze the effect of the R group on the proton affinities of the bases ROH , and to compare the structural changes which occur upon protonation of these bases with those found upon protonation of carbonyl bases;
- (6) to determine the electron redistribution which occurs upon protonation of the bases R_2CO and ROH ;
- (7) to evaluate the effect of mono- and disubstitution of methyl groups on the proton affinities of H_2CO and H_2O , and to compare with experimental data;

(8) to evaluate the severity of the rigid monomer restriction on the computed proton affinities of the bases R_2CO and ROH ; and

(9) to evaluate the reliability of a previously proposed method for computing the relative proton affinities with the 4-31G basis set using optimized STO-3G geometries for the bases and ions.

CHAPTER II

METHOD OF CALCULATIONDetermination of the SCFGround State Wavefunction

In order to describe the electron distribution in a particular system, whether it be a neutral molecule or an ion, it is necessary to determine the wavefunction Ψ for the system.²¹ Ψ is an approximate solution to the Schrödinger equation

$$H\Psi = E\Psi \quad (1)$$

where H is the nonrelativistic Hamiltonian operator

$$H = -\sum_{\mu} \frac{1}{2} \nabla_{\mu}^2 - \sum_A \sum_{\mu} \frac{Z_A}{r_{A\mu}} + \sum_{\mu < \gamma} \frac{1}{r_{\mu\gamma}} + \sum_{A < B} \frac{Z_A Z_B}{r_{AB}} \quad (2)$$

and is composed of electronic kinetic energy, nuclear-electron attraction, and electron-electron and nuclear-nuclear repulsion terms. The energy is calculated as the expectation value

$$\langle E \rangle = \int \Psi^* H \Psi d\tau \quad (3)$$

where the integration is over all space and spin coordinates of all electrons. Since the nuclear motion is slow when compared to the electronic motion, the nuclear repulsion energy is essentially a constant for a given set of nuclear

coordinates and independent of the electron distribution (the Born-Oppenheimer approximation). Therefore, the last term of equation (2) is calculated classically for a particular set of nuclear coordinates.

For a closed shell system, the wavefunction Ψ may be written as a single Slater determinant

$$\Psi = |\psi_1(1)\bar{\psi}_1(2)\psi_2(3)\bar{\psi}_2(4) \dots \psi_n(2n-1)\bar{\psi}_n(2n)| / \sqrt{(2n)!} \quad (4)$$

composed of a set of doubly-occupied molecular orbitals (MO's). The MO's ψ_i are expressed as linear combinations of atomic basis functions ϕ_μ (the LCAO approximation)

$$\psi_i = \sum_{\mu} c_{\mu i} \phi_{\mu} \quad (5)$$

with the coefficients $c_{\mu i}$ determined variationally. The method for obtaining the set of coefficients $c_{\mu i}$ was devised by Roothaan.²² The Roothaan equations may be written in matrix form as

$$FC = SCE \quad (6)$$

or in terms of the matrix elements as

$$\sum_{\gamma} (F_{\mu\gamma} - \epsilon_i S_{\mu\gamma}) c_{\gamma i} = 0 \quad (7)$$

The elements of the matrix representation of the Hartree-Fock Hamiltonian operator F are

$$F_{\mu\gamma} = H_{\mu\gamma} + \sum_{\lambda\sigma} P_{\lambda\sigma} \{ (\mu\gamma|\lambda\sigma) - \frac{1}{2} (\mu\lambda|\gamma\sigma) \} \quad (8)$$

where $H_{\mu\gamma}$ is the one-electron core Hamiltonian

$$H_{\mu\gamma} = \int \phi_{\mu} \left\{ -\frac{1}{2} \nabla^2 - \sum_A \frac{Z_A}{r_{A1}} \right\} \phi_{\gamma} d\tau \quad (9)$$

$(\mu\gamma|\lambda\sigma)$ is the general two-electron interaction integral

$$(\mu\gamma|\lambda\sigma) = \iint \phi_\mu(1)\phi_\lambda(2) \frac{1}{r_{12}} \phi_\gamma(1)\phi_\sigma(2) d\tau_1 d\tau_2 \quad (10)$$

$S_{\mu\gamma}$ is the overlap integral for atomic functions ϕ_μ and ϕ_γ

$$S_{\mu\gamma} = \int \phi_\mu(1)\phi_\gamma(1) d\tau \quad (11)$$

$P_{\lambda\sigma}$ is one of the population elements

$$P_{\lambda\sigma} = 2 \sum_i^{\text{occ}} c_{\lambda i} c_{\sigma i} \quad (12)$$

and ϵ_i is an element of the energy matrix E . If

$$\underline{F}' = \underline{S}^{-\frac{1}{2}} \underline{F} \underline{S}^{-\frac{1}{2}} \quad (13)$$

and

$$\underline{C}' = \underline{S}^{\frac{1}{2}} \underline{C} \quad (14)$$

where $\underline{S}^{\frac{1}{2}}$ is the square root of \underline{S} , then equation (6) may be transformed into the standard form for an eigenvalue problem

$$\underline{F}' \underline{C}' = \underline{C}' \underline{E} \quad (15)$$

The elements ϵ_i of \underline{E} are now the roots of the determinantal equation

$$|F'_{\mu\gamma} - \epsilon \delta_{\mu\gamma}| = 0 \quad (16)$$

\underline{C} can thus be determined from \underline{C}' as

$$\underline{C} = \underline{S}^{-\frac{1}{2}} \underline{C}' \quad (17)$$

The Hartree-Fock matrix elements ($F_{\mu\gamma}$) are dependent upon the orbitals ψ_i via the population elements $P_{\lambda\sigma}$. Thus, to determine these elements and therefore ϵ and E , Ψ must be known. Since the wave function Ψ is to be determined, it is necessary to assume an initial set of linear expansion coefficients $c_{\mu i}$ for the orbitals ψ_i , generate the elements

$P_{\lambda\sigma}$, and compute the elements $F_{\mu\gamma}$. The diagonalization of F is carried out by standard matrix techniques, and yields a new coefficient matrix \underline{C} . The new $c_{\mu i}$'s are then used to recompute F , and the process is repeated until coefficient matrices obtained from two successive iterations are identical within a specified tolerance. At this point the function Ψ is independent of the initial guess, and is comprised of a set of self-consistent molecular orbitals.

In this work, the Roothaan equations are solved within the framework of ab initio MO theory. At this level of theory, all one- and two-electron integrals appearing in the Fock matrix are evaluated exactly in terms of the components of H and the mathematical expressions for the basis functions. Ab initio calculations make no assumptions regarding the nature and magnitude of electron interactions, or the types of atomic hybridization in the molecule. No empirical data are used for the evaluation of integrals associated with the Fock matrix. Therefore, at this more sophisticated level of theory, less biased and thus more reliable information can be obtained about the systems under investigation.

Basis Sets

As noted above, the MO's ψ_i which comprise the Slater determinant are expressed as linear combinations of atomic basis functions ϕ_μ (the LCAO approximation)

$$\psi_i = \sum_{\mu} c_{\mu i} \phi_{\mu} \quad (18)$$

These basis functions describe mathematically the atomic orbitals on the atoms. Either Slater type orbitals (STO's) of the form

$$\phi = Ar^{n-1} e^{-\xi r} \quad (19)$$

or Gaussian orbitals (GTO's)

$$\phi = Br^{\lambda} e^{-\alpha r^2} \quad (20)$$

are commonly employed. For calculations on molecular systems, Slater type orbitals (STO's) are generally preferred, since a given number of STO's provides a better description of a molecular system than the same number of GTO's. However, the calculation of the two-electron integrals with an STO basis set is prohibitive, since numerical integration must be employed. In contrast, these same integrals can be evaluated analytically with a Gaussian basis.

In order to incorporate the best characteristics of both types of functions, Pople and coworkers replaced each Slater type orbital (STO) with a least squares fitted sum of N Gaussian functions. The new basis set, STO-NG, approaches at large N the Slater basis.²³ Studies have been performed on ground and excited states with STO-NG basis sets to determine the value of N best suited for molecular

studies. The results of these studies indicate that the STO-3G basis set represents the level at which computationally consistent results can be obtained with a minimal amount of computing time.²³⁻²⁶ Therefore, the calculations reported here have been performed with the STO-3G basis set. In this minimal basis set, the orbitals of each atom (1s for H, 1s, 2s, 2p_x, 2p_y, and 2p_z, for C, O, N, and F) are described by a set of three Gaussian functions, fitted to the appropriate STO. The standard scale factors proposed by Pople have been used.²³

A second, more flexible basis set has also been employed in this study for the LCAO expansions of the MO's. When the computed STO-3G relative proton affinities were suspect, or in the cases where experimental data were available, additional calculations have been carried out using the extended 4-31G basis set. With this basis set, the inner shell 1s orbital of a first-row atom is represented by a four-term Gaussian function. Each valence shell orbital is described by two independent functions, an inner orbital and a diffuse outer orbital. The inner orbital is represented by three Gaussian functions, while the outer orbital is represented by a single Gaussian. Exponents and coefficients for the 4-31G basis set were determined by Pople and coworkers by minimizing the energy of the ground state atom.²⁷ Again the standard scale

factors proposed by Pople have been used. The splitting of the valence shell into independent inner and outer orbitals provides more flexibility and therefore a more proper description of molecular anisotropy.

Geometry Optimization

Although the STO-3G basis set overestimates the proton affinities of bases,¹⁴⁻¹⁷ the structures of bases and ions predicted by STO-3G calculations are similar to those obtained from 4-31G calculations. More significantly, it has been demonstrated that trends in changes in bond distances and bond angles upon protonation of carbonyl bases are similar at the STO-3G and 4-31G levels.¹⁸ Therefore, the STO-3G basis set has been used to determine the equilibrium (minimum energy) structures of all ions in the series R_2COH^+ . For these ions, C_s symmetry has been assumed, and bond distances and bond angles have been optimized cyclicly and independently to $\pm 0.01\overset{\circ}{\text{Å}}$ and $\pm 1^\circ$, respectively. Parabolic interpolation has been employed to estimate bond distances to $0.001\overset{\circ}{\text{Å}}$ and bond angles to 0.1° . For protonated acetone and protonated carbonic acid, the conformations of the CH_3 and OH groups, respectively, are the same conformations as in the lowest energy structures of the bases.²⁸ However, since the C_s structure is not the lowest energy structure for protonated carbonic acid, an equilibrium C_{3h} structure has also been determined.

The structures and energies of $(CH_3)_2O$ and its ion $(CH_3)_2OH^+$ have been determined with the STO-3G basis set and added to the analysis of substituent effects on the bases ROH and the ions ROH_2^+ whose structures were

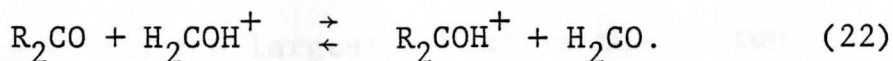
determined by Pople and coworkers.²⁰ In addition, optimized 4-31G structures for the methyl substituted derivatives of H_2O and H_2CO and the corresponding protonated derivatives have been determined with the 4-31G basis set using the same optimization procedure as described for the STO-3G studies. Similarly, the structures and energies of $(\text{HO})_2\text{CO}$ and $\text{C}(\text{OH})_3^+$ have been determined with the 4-31G basis set.

Calculation of Proton Affinities

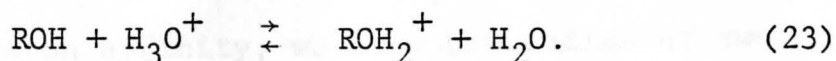
The proton affinity of a base B is the negative energy ($-\Delta E$) for the reaction



ΔE is computed as the difference between the energies of the geometry optimized ion (BH^+) and the base (B). The proton affinity of a disubstituted carbonyl base relative to formaldehyde is expressed as $-\delta\Delta E$, which is the energy of the proton transfer reaction



For the compounds ROH, the proton affinity relative to water is also expressed as $-\delta\Delta E$, which is the energy of the proton transfer reaction

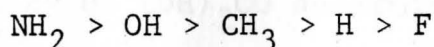


For both series, a positive value of $-\delta\Delta E$ indicates that the proton affinity of the substituted base is greater than that of the reference base, H_2CO or H_2O . All calculations performed in this study have been carried out in double precision on an IBM 370/148 computer.

CHAPTER III

SUMMARYProton Affinities of R₂CO (STO-3G)

The relative proton affinities ($-\delta\Delta E$) of the bases R₂CO determined from fully optimized ions R₂COH⁺ are reported in Table 1. These data show that substitution of two NH₂ groups has the largest effect on the proton affinity, since urea has a proton affinity that is more than 31 kcal/mol higher than any other disubstituted carbonyl base. Substitution of two CH₃, NH₂, or OH groups increases the proton affinity, while substitution of two F atoms decreases the proton affinity relative to formaldehyde. Thus, the STO-3G order of proton affinity of bases R₂CO with respect to R is



with the computed proton affinities of acetone and carbonic acid differing by only 2.2 kcal/mol. This is the same order predicted for the bases RCHO with this basis set.¹⁸

However, it was observed in the study of the bases RCHO that the prediction that formic acid has a higher proton affinity than acetaldehyde is contrary to experimental data,² and to the order predicted from 4-31G calculations.¹⁹

It appears that the STO-3G basis set tends to underestimate the electronegativity of the OH group in these ions, and to

TABLE 1
Relative Proton Affinities of Substituted Carbonyl
Compounds (STO-3G)^a

	R ₂ CO		RCHO ^b	
	- $\delta\Delta E$		- $\delta\Delta E(A)$ ^c	- $\delta\Delta E(B)$ ^c
R=H	0.0		0.0	0.0
CH ₃	27.9		15.3	15.3
NH ₂	61.3		41.9	38.9
OH	21.1	(30.1) ^d	17.7	11.4
F	-6.4		-2.1	-0.8

- a) In kcal/mol. Based on a computed proton affinity of 221.3 kcal/mol for H₂CO.
- b) Data for RCHO taken from ref. 18.
- c) Ions in set A have the proton trans to R with respect to the CO bond. Those in set B have the proton cis to R.
- d) Proton affinity of (OH)₂CO determined from the ion of C_{3h} symmetry.

overestimate the amount of charge transfer to the proton.^{18,29} Therefore, the analogous STO-3G prediction that the proton affinity of carbonic acid is greater than that of acetone is suspect, and has been further investigated using the 4-31G basis set. The results of these studies are presented in the section on the 4-31G proton affinities.

The effect of mono- vs. disubstitution on the proton affinities of carbonyl bases can be determined by comparing the relative proton affinities of bases R_2CO with the relative proton affinities of bases $RCHO$. To make this comparison for formic and carbonic acids, it is necessary to refer to the carbonic acid ion having C_s symmetry so that the relative H atom positions in this ion correspond to the positions in cis and trans protonated formic acid. It is apparent from the data of Table 1 that whether the substituent R increases or decreases the proton affinity of $RCHO$ relative to H_2CO , the second substituent leads to a further change in the proton affinity of R_2CO in the same direction. For substituents CH_3 , NH_2 , and OH , substitution of one R group increases the proton affinity of $RCHO$ relative to H_2CO . Substitution of the second R group further increases the proton affinity, although the effect of two substituents is less than additive. Unlike CH_3 , NH_2 , and OH , F substitution lowers the proton affinity of $HFCO$ relative to H_2CO . Disubstitution leads to a further

reduction of the proton affinity of F_2CO , and only in this case is the effect of the two substituents more than additive. This may be due to the fact that in $HFCOH^+$, it is the H atom on the carbon which loses a large amount of electron density as charge is transferred to the proton. In fact, the amount of negative charge lost by H is greater in $HFCOH^+$ than in any other ion of the series, due to the high electronegativity of F. Replacement of the H atom by a second F does not facilitate charge transfer to the proton, which stabilizes protonated bases. Hence, the presence of two F atoms decreases the amount of charge transfer, and therefore significantly lowers the proton affinity of F_2CO .

Mulliken population analyses³⁰ have been employed to describe the effect of protonation on the electron redistribution in the ions R_2COH^+ . The population data of Table 2 show that the amount of electron transfer to the proton tends to increase as the proton affinity of the base increases. However, charge transfer is slightly less in H_2COH^+ than in F_2COH^+ , even though F_2CO has the lower proton affinity. The larger charge transfer in F_2COH^+ is most probably a result of the underestimation of the electronegativity of F by the STO-3G basis set.

Charge transfer to the proton occurs in the symmetry plane of the ion, and is accompanied by an increased polarization of the π electron cloud toward and within the carbonyl group. As a result, the carbonyl oxygen remains

TABLE 2

Mulliken Population Data for R_2COH^+ (STO-3G)

R_2COH^+	Oxygen Electron Population ^a	Electron Transfer to H^+	Electron Loss by CO	Pi Electron Gain by CO
R=H	8.117 (8.188)	0.617	0.280	0.0
CH ₃	8.164 (8.226)	0.662	0.233	0.072
NH ₂	8.212 (8.319)	0.706	0.208	0.322
OH ^b	8.211 (8.300)	0.678	0.265	0.277
F	8.160 (8.236)	0.623	0.313	0.176

a) Data in parentheses are oxygen electron populations in the bases.

b) Data for protonated carbonic acid are for the C_s structure.

negatively charged in the ions. It is apparent that for those bases which have high proton affinities, the electron density lost by the carbonyl group is minimized due to the donation of electron density by the substituents to the carbonyl group. A good example is protonated urea, where charge transfer to the proton is greatest, yet the CO group loses the smallest amount of electron density due to π electron donation by the NH_2 groups. Thus, the ability of the substituent to donate electrons to the carbonyl group is an important factor in determining the relative proton affinities of carbonyl bases. In this respect it should be noted that it is not accidental that in ions having high proton affinities and π donating substituents, large decreases in the bond length from the carbon to the substituent have been found, since a shortening of this bond facilitates π electron donation.

Structures of R_2COH^+ (STO-3G)

The STO-3G equilibrium structures of the bases R_2CO ³¹ and of the corresponding fully optimized ions R_2COH^+ are reported in Table 3 and the ion structures are illustrated in fig. 1. Except for protonated carbonic acid which has C_{3h} symmetry, the equilibrium structures of these ions have C_s symmetry. For protonated carbonic acid, the ion of C_s symmetry will first be examined in the analysis of structural changes caused by protonation of carbonyl bases, since in this ion, the conformations of the OH groups are the same as in the base.

It is apparent from Table 3 that protonation leads to an increase in the carbonyl C-O bond length. This increase varies from 0.072 $\overset{\circ}{\text{A}}$ in protonated acetone to 0.126 $\overset{\circ}{\text{A}}$ in protonated urea. These increases are larger than the 0.054 $\overset{\circ}{\text{A}}$ increase in protonated formaldehyde. As in the monosubstituted carbonyls, protonation causes a much greater variation in the C-O bond length in the ions R_2COH^+ than in the bases R_2CO . The increase in the carbonyl C-O bond length in ions R_2COH^+ suggests that protonation weakens the C-O bond. This is supported by the data in Table 4 obtained from Mulliken population analyses which indicate that the total and π C-O overlap populations decrease in the ions relative to the corresponding bases, and it is also consistent with experimental data which show that complexation of carbonyl compounds with Lewis acids leads to lower C-O stretching frequencies.³²

TABLE 3

Structures of Bases R_2CO and Ions R_2COH^+ (STO-3G)^a

		Base ^b	Ion	
R_2COH^+ R=H ^c	CO	1.217	1.271	
	CH _a	1.101	1.114	
	CH _b	1.101	1.114	
	R		1.003	
	OCH _a	122.8	116.4	
	OCH _b	122.8	123.0	
	θ		114.7	
	CH ₃	CO	1.219	1.291
		CC _a	1.543	1.526
		C _a H' ^d	1.086	1.090
CC _b		1.543	1.524	
C _b H' ^e		1.086	1.090	
R			0.997	
OCC _a		122.3	115.9	
CC _a H'		109.9	110.1	
H'C _a H'' ^d		108.8	110.1	
OCC _b		122.3	122.3	
CC _b H'		109.9	112.1	
H'C _b H'' ^e		108.8	109.4	
θ			113.0	

NH ₂	CO	1.222	1.348
	CN _a	1.412	1.343
	N _a H'	1.013	1.024
	N _a H''	1.012	1.022
	CN _b	1.412	1.350
	N _b H'	1.013	1.023
	N _b H''	1.012	1.022
	R		0.991
	OCN _a	123.7	114.8
	CN _a H'	119.0	119.0
	CN _a H''	122.6	122.1
	OCN _b	123.7	123.0
	CN _b H'	119.0	121.6
	CN _b H''	122.6	120.7
	θ		109.3
	OH ^f	CO	1.216
CO _a		1.385	1.320
O _a H'		0.990	0.996 (0.995)
CO _b		1.385	1.327
O _b H'		0.990	0.994
R			0.993
OCO _a		125.8	117.8 (120.0)
CO _a H'		104.2	109.2 (110.0)
OCO _b		125.8	128.2
CO _b H'		104.2	111.8
θ			112.8

F	CO	1.209	1.299
	CF _a	1.347	1.300
	CF _b	1.347	1.306
	R		1.001
	OCF _a	125.0	118.2
	OCF _b	125.0	123.6
	θ		112.8

- a) Bond lengths in Å, bond angles in degrees. See fig. 1 for labeling of atoms.
- b) Structures of bases R₂CO taken from ref. 31.
- c) Data for H₂CO and H₂COH⁺ taken from ref. 18.
- d) Methyl C_aH bonds and HC_aH angles assumed equal.
- e) Methyl C_bH bonds and HC_bH angles assumed equal.
- f) Data in parentheses are for the ion of C_{3h} symmetry.

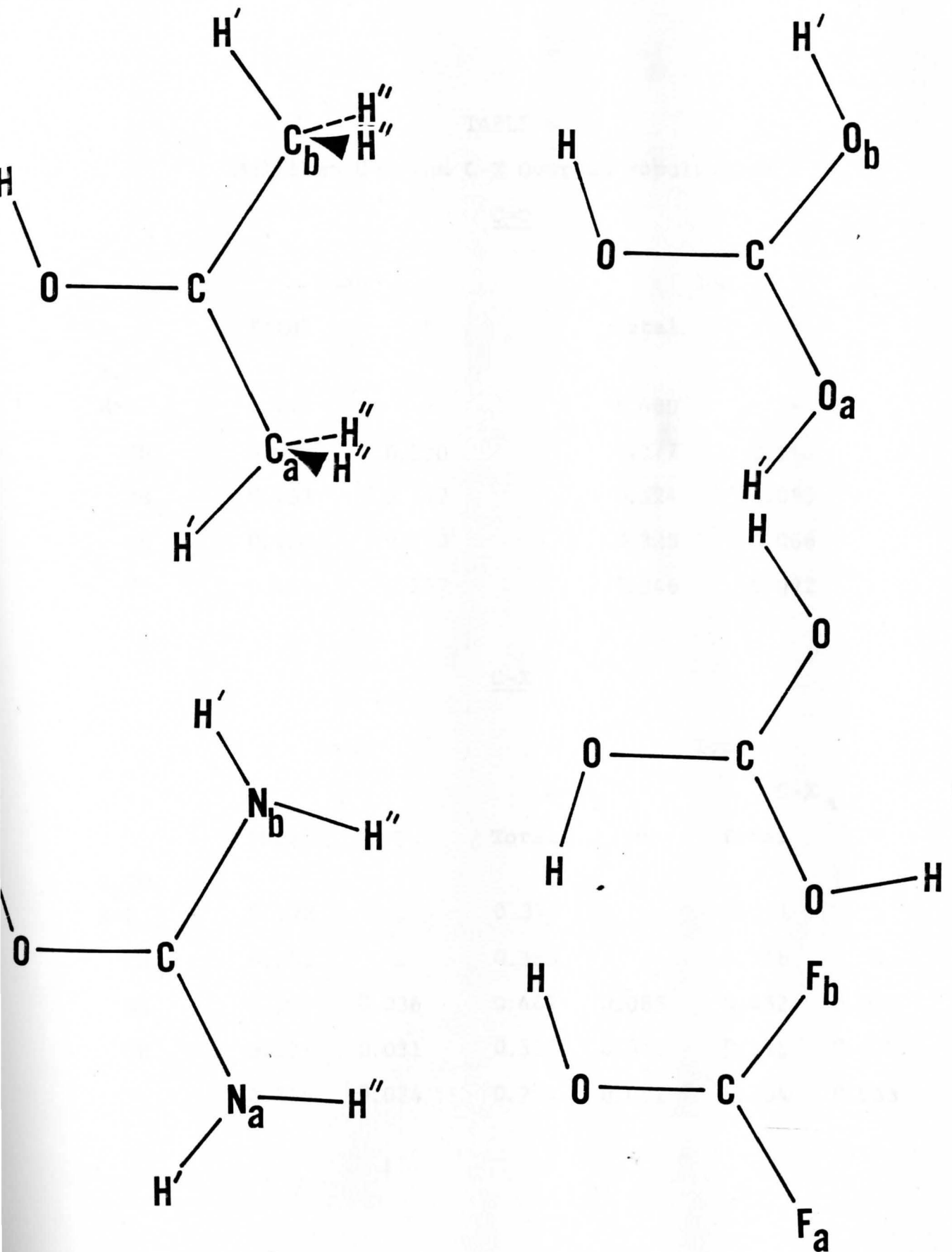


Figure 1. Equilibrium Structures of R_2COH^+

TABLE 4

Mulliken C-O and C-X Overlap Populations

	<u>C-O</u>			
	Base		Ion	
	Total	π	Total	π
R_2CO				
R=H	0.444	-	0.400	-
CH ₃	0.443	0.170	0.377	0.114
NH ₂	0.433	0.147	0.324	0.055
OH	0.424	0.150	0.320	0.066
F	0.429	0.157	0.346	0.092

	<u>C-X</u>					
	Base			Ion		
	Total	π	C-X _b		C-X _a	
Total			π	Total	π	
R_2CO						
R=H	0.372	-	0.370	-	0.371	-
CH ₃	0.353	-	0.360	-	0.358	-
NH ₂	0.366	0.036	0.441	0.085	0.452	0.091
OH	0.273	0.031	0.330	0.070	0.341	0.075
F	0.214	0.024	0.244	0.051	0.254	0.053

A comparison of the C-O bond lengths in R_2COH^+ and $RCHOH^+$ shows that the C-O bond is longer in R_2COH^+ than in the corresponding ions $RCHOH^+$, just as the C-O bond is longer in R_2CO than in $RCHO$. Moreover, the C-O bond length increases to a greater extent upon protonation of R_2CO than upon protonation of the corresponding base $RCHO$, even when the proton affinity of R_2CO is less than $RCHO$, as when R is F. In addition, the C-O total and π overlap populations are smaller in R_2COH^+ than in the corresponding ions $RCHOH^+$ except when R is CH_3 , in which case the C-O overlap population is slightly greater in cis protonated acetaldehyde. Therefore, it appears that except when R is CH_3 , protonation weakens the C-O bond in a disubstituted carbonyl base to a greater extent than in the corresponding monosubstituted carbonyl base.

Protonation may also lead to a decrease in the C-X bond length (X is the first-row atom of the substituent bonded to the carbonyl carbon) in ions R_2COH^+ relative to the corresponding bases R_2CO . The amount of decrease depends upon the substituent and varies from $0.017\overset{\circ}{\text{A}}$ and $0.019\overset{\circ}{\text{A}}$ for the C-C bonds trans and cis to the proton ($C-C_a$ and $C-C_b$, respectively, see fig. 1) in protonated acetone, to $0.062\overset{\circ}{\text{A}}$ and $0.069\overset{\circ}{\text{A}}$ for the $C-N_b$ and $C-N_a$ bonds, respectively, in protonated urea. As evident from Table 3, protonation leads to similar changes in the two C-X bond lengths independent of whether the C-X bond is cis or trans

to the proton. However, the $C-X_a$ bond does decrease to a slightly greater extent than the $C-X_b$ bond in all cases except protonated acetone. The maximum difference between the $C-X_a$ and $C-X_b$ bond lengths is only $0.007\overset{\circ}{\text{A}}$, the difference in the C-N bond lengths in protonated urea. The decrease in these bond lengths suggests that the C-X bonds in the ions are stronger than in the corresponding bases. This is also supported by the Mulliken population data in Table 4, which show that the total (and for ions having separable π systems, the π) overlap populations increase in R_2COH^+ relative to R_2CO , with a greater increase occurring in the $C-X_a$ populations in all cases except protonated acetone. In this ion, there is a slightly greater decrease in the $C-C_b$ bond distance (by $0.002\overset{\circ}{\text{A}}$) and a corresponding increase in the $C-C_b$ overlap population relative to $C-C_a$.

It is interesting to note that the C-X bond lengths in the ions R_2COH^+ are longer than the C-X bond lengths in the corresponding ions $RCHOH^+$, just as the C-X bonds in R_2CO are longer than the C-X bond in the corresponding base $RCHO$. Moreover, the change in the C-X bond lengths upon protonation of a disubstituted carbonyl base is less than that found upon protonation of the corresponding monosubstituted carbonyl base. It is not surprising that the two C-X bond lengths in R_2COH^+ do not contract to the extent found in $RCHOH^+$ since in the former, both R groups may

donate electrons to CO, and the shortening of the C-X bonds facilitates this donation. As anticipated, both the total and the π (in ions having separable π electron systems) C-X overlap populations are smaller in R_2COH^+ than in the corresponding ions $RCHOH^+$ except when R is CH_3 , in which case the total C-C overlap populations are similar.

The position of the proton relative to the carbonyl group is described by the protonation coordinates R, the O-H bond length, and θ , the H-O-C angle. From the data of Table 3, it is apparent that the O-H bond length in R_2COH^+ is essentially independent of the substituent and therefore of the proton affinity of the base. In the two series of ions $RCHOH^+$ and R_2COH^+ , the O-H bond length varies only from $0.991\overset{\circ}{\text{Å}}$ in protonated urea to $1.003\overset{\circ}{\text{Å}}$ in protonated formaldehyde. In addition, the angle θ exhibits only a small variation in both series of ions, from 109.3° in protonated urea to 114.7° in protonated formaldehyde. Thus, the protonation coordinates R and θ show little dependence on the nature of the substituent and on the presence of one or two R groups bonded to the carbonyl carbon. The constancy of the coordinates R and θ indicates that the bond between the proton and the carbonyl oxygen has the structural characteristics of a normal intramolecular covalent bond.

Unlike changes in bond distances, changes in the O-C-X bond angles show a dramatic dependence on the proton position relative to the substituent. In ions R_2COH^+ , the O-C-X_a angle decreases significantly (by 6 to 10°) upon protonation of R_2CO . By contrast, only a small change in the O-C-X_b angle occurs in R_2COH^+ relative to R_2CO . The largest change in ions of C_s symmetry is found in protonated carbonic acid, where the O-C-X_b angle increases by 2.4°. This is probably a direct result of the repulsion between the nearby O-H groups (see fig. 1). From changes in the O-C-X_a and O-C-X_b angles, it is apparent that the X_a-C-X_b angle must increase in the ion relative to the base.

The changes in bond angles about the carbonyl carbon in ions R_2COH^+ are analogous to the changes found in $RCHOH^+$. In these ions, the O-C-X or O-C-H angles trans to the proton decrease, while the O-C-X or O-C-H angles cis to the proton change only slightly, resulting in an increase in the X-C-H angle. Thus it appears that these angular changes about the carbon resulting from oxygen protonation of carbonyl bases are essentially independent of the atoms bonded to the carbon.

As noted previously, the conformation of the OH groups in the protonated carbonic acid ion of C_s symmetry is the most favorable conformation determined for the base. In this conformation, the two O-H bonds are s-cis to the C-O double bond with respect to the C-O single bonds,

as shown in fig. 1. Protonation then leads to a structure in which the proton added to the carbonyl oxygen and the hydroxyl hydrogen bonded to O_b approach each other, and this has a destabilizing effect on the ion. The repulsion between these two hydrogens can be relieved if the O_b-H bond rotates 180° about the $C-O_b$ bond. Optimization of an ion with this conformation leads to the most stable structure for protonated carbonic acid, which has C_{3h} symmetry. In this ion, the C-O and O-H bond lengths are $1.322\overset{\circ}{\text{A}}$ and $0.995\overset{\circ}{\text{A}}$, respectively, and the C-O-H angles are 110.0° . Of course the O-C-O angles are 120° , by symmetry. It is interesting to note that the values of the C-O and O-H bond lengths and of the C-O-H angles in this ion are similar to those in the optimized carbonic acid ion having C_s symmetry.

The Rigid Monomer Restriction in R_2COH^+ (STO-3G)

To make studies of proton affinities of bases more tractable by reducing computer time, various investigators have applied some form of a rigid monomer (rigid base) restriction to protonated ions. This restriction consists of freezing the geometry of the base, and optimizing only the protonation coordinates R and θ in the ion. However, it has been demonstrated that this is a severe restriction in ions $RCHOH^+$.¹⁸ The severity of the rigid monomer restriction will now be examined in the ions R_2COH^+ .

The relative proton affinities of the bases R_2CO determined using the rigid monomer restriction for the ions R_2COH^+ ($-\delta\Delta E_r$) are reported in Table 5 in conjunction with the relative proton affinities determined from the fully optimized ions R_2COH^+ ($-\delta\Delta E_f$). Relaxation of the rigid monomer restriction naturally leads to larger computed proton affinities. The rigid monomer restriction is more severe in R_2CO than in H_2CO whether the proton affinity of R_2CO is greater or less than that of H_2CO , and is strongly dependent on the substituent. It is most severe when R is OH , where it leads to an underestimation of the computed proton affinity of carbonic acid by 25.3 kcal/mol relative to the fully optimized ion. This is due to the fact that the fully-optimized equilibrium structure of

TABLE 5

The Effect of the Rigid Monomer Restriction on the Computed Relative Proton Affinities of R_2CO (STO-3G)^a

R_2CO	$-\delta\Delta E_r^b$	$-\delta\Delta E_f^c$
R=H	0.0	0.0
CH ₃	25.1	27.9
NH ₂	46.5	61.3
OH	8.9	30.1
F	-13.0	-6.4

a) In kcal/mol.

b) Based on a computed proton affinity of 217.2 kcal/mol for H_2CO .

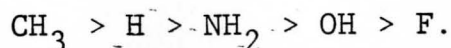
c) Based on a computed proton affinity of 221.3 kcal/mol for H_2CO .

protonated carbonic acid has C_{3h} symmetry, and therefore three equivalent C-O and O-H bonds. It is much less severe when R is CH_3 since the computed proton affinity of acetone increases by 6.9 kcal/mol when the rigid monomer restriction is relaxed. As a result of these differences, the predicted relative proton affinities of acetone and carbonic acid are reversed when the rigid monomer restriction is relaxed. Thus, even relative proton affinities of related bases are suspect when computed with the rigid monomer restriction.

The severity of the rigid monomer restriction appears to be directly related to the change in the length of the C-X bond upon protonation. When the C-X bond length decreases significantly, as in protonated carbonic acid and protonated urea, the computed relative proton affinity of the base is dramatically changed upon relaxation of the rigid monomer restriction. When there is only a small decrease in the C-X distance as in protonated acetone, the rigid monomer restriction is not so severe, and provides a more reasonable estimate of the proton affinity of the base relative to H_2CO .

Proton Affinities of ROH (STO-3G)

The optimized STO-3G structures of the bases ROH and of the ions ROH_2^+ have been reported by Pople and co-workers in a comprehensive study of structures H_mABH_n ,²⁰ but no analyses of these structures or of the computed proton affinities were made. Therefore, in this work, an analysis of substituent effects on the proton affinities of bases ROH and of the structures of ions ROH_2^+ has been carried out. The computed relative proton affinities of the bases ROH are reported in Table 6. As evident from these data, the predicted order of proton affinity of bases ROH with respect to R is



This order is dramatically different from the order of proton affinity of mono- and disubstituted carbonyls, where only F substitution leads to a decrease in the proton affinity relative to the unsubstituted base.

The substituents R in the bases ROH are electron withdrawing groups relative to H. However, upon protonation of bases ROH, the R group becomes an electron donating group to reduce the positive charge on the OH_2 group. Among the substituents, only CH_3 donates more electron density to this group than does H. That electron donation by the substituent is an important factor in determining the stability of the ions ROH_2^+ and therefore

TABLE 6

Relative Proton Affinities of Bases ROH (STO-3G)^a

	Computed Subject to the Rigid Monomer Restriction	Computed from the Fully Optimized Ions
ROH	$(-\delta\Delta E_r)^b$	$(-\delta\Delta E_f)^c$
R=H	0.0	0.0
CH ₃	8.3	10.0
NH ₂	-3.7	-3.2
OH	-7.7	-9.3
F	-30.0	-31.9

a) In kcal/mol.

b) Based on a computed proton affinity of 224.7 kcal/mol for H₂O.

c) Based on a computed proton affinity of 228.7 kcal/mol for H₂O.

the proton affinities of the bases ROH is demonstrated by the correlation between the total electron populations of the OH_2 group as determined by Mulliken population analyses (Table 7), and the relative proton affinities of the bases ROH, which are found to decrease in the same order. Thus, it appears that the ability of the R group to donate electrons through the O-X bond (X is the first row atom of the substituent bonded to the oxygen) is an important factor in determining the relative proton affinities of these bases.

Protonation also causes electron density to be lost by the OH proton in the base. Electron density loss by this hydrogen is greatest upon protonation of FOH, due to the high electronegativity of fluorine, which does not readily donate electrons even to relieve the positive charge in the OH_2 group. To compensate, electron density must flow from the hydrogen of FOH to be redistributed in the OH_2 group. There is an inverse relationship between the electron density lost by the R group upon protonation of the base and the electron density lost by the hydrogen atom in the base. The greater the tendency for R to retain electron density, the more electron density lost by this H atom. This relationship is evident from the data of Table 7.

TABLE 7

Mulliken Population Data for Bases ROH and Ions ROH₂⁺ (STO-3G)^a

	Oxygen Electron Density	Hydrogen Electron Density	Electron Density in OH ₂	Electron Density in R Group	O-X Overlap _b Population
ROH					
R=H	8.257 (8.330)	0.581 (0.835)	9.419	0.581 (0.835)	0.282 (0.254)
CH ₃	8.218 (8.280)	0.614 (0.826)	9.446	8.552 (8.894)	0.234 (0.263)
NH ₂	8.163 (8.223)	0.610 (0.805)	9.383	8.617 (8.971)	0.177 (0.215)
OH	8.137 (8.189)	0.597 (0.811)	9.331	8.669 (9.000)	0.148 (0.172)
F	8.079 (8.148)	0.572 (0.804)	9.223	8.778 (9.048)	0.134 (0.142)

a) Data in parentheses refer to the bases ROH.

b) X is the first row atom of the R group.

Structures of ROH₂⁺ (STO-3G)

The structures of the ions ROH₂⁺ are reported in Table 8 and illustrated in fig. 2. The equilibrium structures of the bases ROH are also reported in Table 8. As evident from these data, oxygen protonation leads to an increase in the O-X bond length. The largest increases are found in the C-O distance in CH₃OH₂⁺ and in the N-O distance in NH₂OH₂⁺ where changes of 0.052Å and 0.056Å, respectively, occur upon protonation. In HOOH₂⁺ and FOH₂⁺, smaller changes of 0.032Å and 0.016Å in the F-O and O-O distances, respectively, occur. There is not a good correlation between increasing proton affinity and increasing O-X bond distance, although larger increases in the O-X distance do occur upon protonation of CH₃OH and NH₂OH, both of which have relatively high proton affinities, and smaller increases occur upon protonation of HOOH and FOH, which have relatively low proton affinities among the ROH compounds.

The results of Mulliken population analyses reported in Table 7 show that the O-X overlap population decreases upon protonation, which suggests a weakening of the O-X bond. There is obviously a correlation between the change in the O-X overlap population and the change in the O-X bond distance upon protonation. In protonated CH₃OH and NH₂OH, ions which experience a significant lengthening of the O-X bonds, the overlap populations decrease significantly.

TABLE 8

Structures of Bases ROH and Ions ROH₂⁺ (STO-3G)^a

		Base	Ion
ROH			
R=H	OH	0.990	0.990
	HOH	100.0	113.9
CH ₃	CO	1.433	1.485
	CH'	1.092	1.096 ^d
	CH''	1.095	
	OH	0.991	0.990
	OCH'	107.7	108.6
	H''CH''	108.1	111.9 ^d
	OCb ^b	130.4	
	COH	103.8	
	COb ^c		139.4
	HOH		110.7
NH ₂	NO	1.427	1.483
	NH	1.044	1.055
	OH	0.995	0.998
	ONb ^b	113.8	108.5
	HNH	103.3	105.1
	NOH	101.4	
	NOb ^c		123.1
	HOH		107.4

OH	OO	1.396	1.428
	OH	1.001	1.002
	OH'	1.001	1.015
	OOH'	101.1	99.7
	HOOH'	125.3	
	HOH		109.5
	OOb ^c		125.4
F	FO	1.355	1.371
	OH	1.006	1.011
	HOF	101.4	
	HOH		112.2
	FOb ^c		128.3

- a) Structural data reported in ref. 20.
- b) Angle between the O-X bond and the bisector of the H-X-H angle.
- c) Angle between the O-X bond and the bisector of the H-O-H angle.
- d) C-H distances and H-C-H angles in the ion assumed equal.

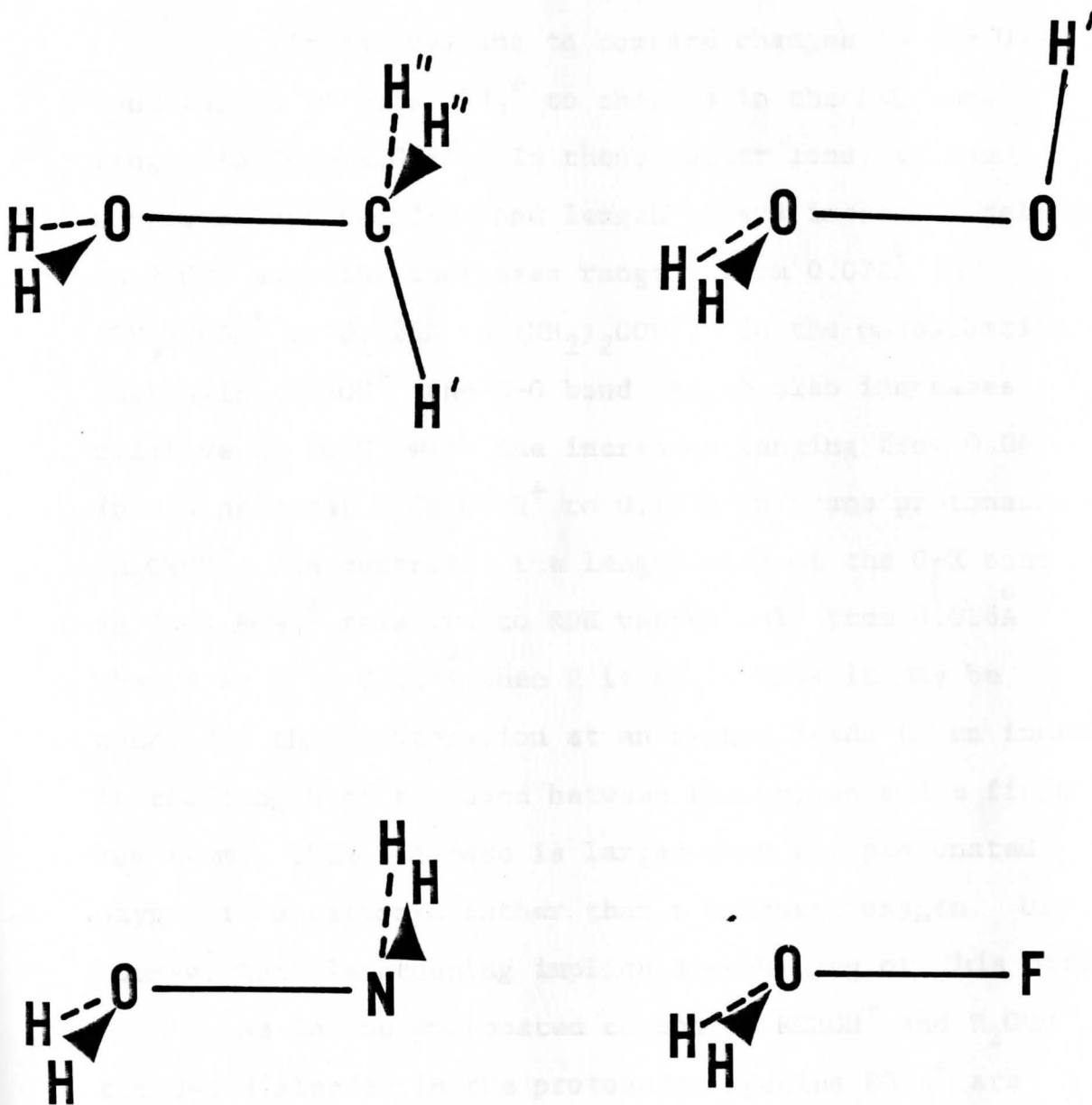


Figure 2. Equilibrium Structures of ROH_2^+

In protonated HOOH and FOH, there is only a slight lengthening of the O-X bond and the overlap populations show only small decreases upon protonation.

It is interesting to compare changes in the O-X bond length in ions ROH_2^+ to changes in the C-O bond length in ions R_2COH^+ . In these latter ions, it was observed that the C-O bond length always increases relative to R_2CO , with the increases ranging from 0.072\AA in $(\text{CH}_3)_2\text{COH}^+$ to 0.126\AA in $(\text{NH}_2)_2\text{COH}^+$. In the monosubstituted carbonyls, RCHOH^+ , the C-O bond length also increases relative to RCHO , with the increases ranging from 0.062\AA in cis protonated CH_3CHOH^+ to 0.105\AA in trans protonated NH_2CHOH^+ . In contrast, the lengthening of the O-X bond in ions ROH_2^+ relative to ROH varies only from 0.016\AA when R is F to 0.056\AA when R is NH_2 . Thus it may be concluded that protonation at an oxygen leads to an increase in the length of the bond between the oxygen and a first row atom. This increase is larger when the protonated oxygen is a carbonyl rather than a hydroxyl oxygen. Of course, this lengthening implies a weakening of this bond.

As in the protonated carbonyls RCHOH^+ and R_2COH^+ , the O-H distances in the protonated species ROH_2^+ are relatively constant, independent of the substituent. The O-H distance varies from 0.990\AA in protonated water and protonated methanol to 1.011\AA in protonated HOF.

The H-O-H angle also shows a relatively small variation from 107.4° in NH_2OH_2^+ to 112.2° in FOH_2^+ . The X-O-b angle, which is the angle between the O-X bond and the H-O-H plane, is also relatively constant, ranging from 123.1° to 128.3° except in CH_3OH_2^+ , where it has a significantly larger value of 139.4° . This increase is probably due to the repulsion between the in-plane hydrogen of the methyl group (H' of fig. 2) and the hydrogens bonded to the oxygen. It is interesting to note that the H-O-b angle in hydronium ion is also large (138°), due to the repulsion between the hydrogens.

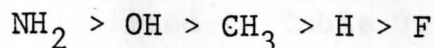
The Rigid Monomer Restriction in ROH_2^+ (STO-3G)

It is appropriate to evaluate the severity of the rigid monomer restriction on the computed relative proton affinities of bases ROH. This can be done by comparing the relative proton affinities of the ROH compounds computed from the fully optimized ions ($-\delta\Delta E_f$) to the relative proton affinities computed subject to the rigid monomer restriction ($-\delta\Delta E_r$), as reported in Table 6. As expected, relaxation of the rigid monomer restriction leads to larger computed proton affinities. The rigid monomer restriction is most severe when R is CH_3 and NH_2 , since relaxation of this restriction increases the computed proton affinities of CH_3OH and NH_2OH by 5.7 and 4.5 kcal/mol, respectively. The error introduced by the rigid monomer restriction arises primarily from neglecting the large increase in the C-O and N-O bond distances in these ions. The rigid monomer restriction is less severe in HOOH_2^+ and FOH_2^+ since relaxation of this restriction leads to increases in the computed proton affinities of HOOH and FOH of only 2.4 and 2.1 kcal/mol, respectively. In these ions, only small increases in the O-O and F-O distances occur upon protonation. The order of proton affinity of ions ROH_2^+ remains the same whether the rigid monomer restriction is in effect or has been relaxed. Thus it is apparent that the rigid monomer restriction is

less severe in ROH_2^+ than in R_2COH^+ . It is also interesting to note that the rigid monomer restriction is most severe in ions ROH_2^+ when R is CH_3 , but least severe in ions R_2COH^+ when R is CH_3 . This suggests that although ions in both series are stabilized through electron transfer to the proton facilitated by electron donation from the substituent, the mechanism by which this occurs is quite different in these two series of ions.

Proton Affinities (4-31G)

The STO-3G calculations predict that the order of proton affinity of bases R_2CO with respect to R is



with the computed proton affinities of acetone and carbonic acid differing by only 2.2 kcal/mol. However, for the bases RCHO, the STO-3G prediction that formic acid has a higher proton affinity than acetaldehyde is contrary to experimental data² and to the order predicted from the 4-31G calculations.¹⁹ It appears that the STO-3G basis set tends to overestimate the amount of charge transfer to the proton and to underestimate the electronegativity of the OH group in protonated carbonyls. Therefore, for the bases R_2CO , the proton affinities of acetone and carbonic acid have been further investigated using the extended 4-31G basis set.

As anticipated, the 4-31G basis set calculations predict a reversal in the relative proton affinities, with acetone having a proton affinity higher than that of carbonic acid by 13.2 kcal/mol. The relative proton affinities of H_2CO , $(HO)_2CO$, and $(CH_3)_2CO$ ($-\delta\Delta E$) are 0.0, 9.9, and 23.1 kcal/mol, respectively. These 4-31G results and those reported in reference 18, combined with the STO-3G relative proton affinities lead to a predicted order of proton affinity for the bases R_2CO with respect to R of



which is the same order predicted for the bases RCHO.

Ion Structures (4-31G)

The 4-31G equilibrium structures of acetone and protonated acetone, and carbonic acid and protonated carbonic acid (C_{3h}) are listed in Table 9. It is apparent from this table that protonation of these bases leads to increases in the carbonyl C-O bond lengths, although the increase at the 4-31G level is not as great as predicted from the STO-3G calculations. A comparison of the structures of acetone and protonated acetone shows that protonation also leads to small decreases in the C-C bond lengths, which are only slightly dependent on whether the C-C bond is cis or trans to the proton. Unlike changes in bond distances, changes in the O-C-C bond angles in protonated acetone show a dependence on the proton position relative to the two C-C bonds. In protonated acetone, the $O-C-C_a$ angle decreases by 5.5° while only a small change of 0.2° occurs in the $O-C-C_b$ angle, and the C_a-C-C_b angle increases in the ion relative to the base. Therefore, the major structural changes which occur upon protonation of acetone are evident when computed with both the STO-3G and 4-31G basis sets.

To compare the 4-31G proton affinities of H_2O , CH_3OH , and $(CH_3)_2O$, it was first necessary to determine the equilibrium structures of methanol and dimethyl ether and the corresponding ions with the 4-31G basis set.

TABLE 9

Equilibrium Structures of Acetone,
Carbonic Acid, Protonated Acetone,
and Protonated Carbonic Acid (4-31G)^a

		Base	Ion
$(\text{CH}_3)_2\text{CO}^b$	CO	1.213	1.273
	CC _a	1.506	1.475
	C _a H	1.082	1.082
	CC _b	1.506	1.478
	C _b H	1.082	1.083
	R		0.962
	OCC _a	121.5	116.0
	CC _a H'	109.5	111.0
	H'C _a H''	108.9	108.8
	OCC _b	121.5	121.7
	CC _b H'	109.5	113.5
	H'C _b H''	108.9	108.4
	θ		122.3
	$(\text{OH})_2\text{CO}^c$	CO	1.207
CO _a		1.328	1.274
O _a H		0.955	0.964
OCO _a		124.9	120.0
CO _a H		113.5	121.3

a) Bond lengths in Å, bond angles in degrees. See fig. 1.

b) See footnotes d and e of Table 3.

c) Data for the ion of C_{3h} symmetry.

The equilibrium structures of these bases and ions are reported in Table 10 along with the structures of H_2O and H_3O^+ , which have been determined by Newton and Ehrenson.¹⁴ As evident from comparing the 4-31G structures reported in Table 10 with the corresponding STO-3G structures in Tables 8 and 11, oxygen protonation leads to similar increases in the O-H and C-O bond lengths when computed with both basis sets. However, it should be noted that unlike the STO-3G basis set, the 4-31G basis set tends to flatten the pyramidal angles about the oxygen to the extent that for hydronium ion and protonated dimethyl ether, the three atoms bonded to the oxygen are coplanar, so that the ions have D_{3h} and C_{2v} symmetry, respectively. While protonated CH_3OH has only C_s symmetry, the O-H protons are only 3.8° away from being coplanar with the O and C atoms.

TABLE 10

Equilibrium Structures of H_3O^+ , CH_3OH_2^+ , and
 $(\text{CH}_3)_2\text{OH}^+$ and Their Bases (4-31G)^a

		Base	Ion
$\text{H}_2\text{O}^{\text{b}}$	OH	0.950	0.964
	HOH	111.3	120.0
$\text{CH}_3\text{OH}^{\text{c}}$	CO	1.430	1.535
	CH	1.080	1.073
	OH	0.951	0.959
	OCH'	106.3	106.6
	H' 'CH' '	109.1	113.2
	COH	113.3	
	COb ^d		176.2
	HOH		116.5
$(\text{CH}_3)_2\text{O}^{\text{e}}$	CO	1.421	1.499
	OH		0.956
	CH	1.082	1.074
	OCH'	107.0	106.6
	COC	116.0	122.4
	H' 'CH' '	109.1	112.2
	HObe		180.0

a) Bond lengths in Å, bond angles in degrees. See figs. 2 and 3.

b) Data taken from ref. 14.

c) Computed in this work.

d) Angle between the O-C bond and the bisector of the H-O-H angle.

e) Angle between the O-H bond and the bisector of the C-O-C angle.

TABLE 11
 Equilibrium Structures of $(\text{CH}_3)_2\text{O}$ and
 $(\text{CH}_3)_2\text{OH}^+$ (STO-3G)^a

		Base	Ion
$(\text{CH}_3)_2\text{O}$	CO	1.432	1.475
	CH' ^b	1.094	1.095
	OH		0.990
	COC	109.5	118.3
	H'CH'' ^b	108.2	111.3
	OCH'	107.8	107.1
	HO ^b ^c		138.1

- a) Bond lengths in Å, bond angles in degrees.
 See fig. 3.
- b) All C-H bond lengths and H-C-H angles assumed equal.
- c) Angle between the O-H bond and the bisector of the C-O-C angle.

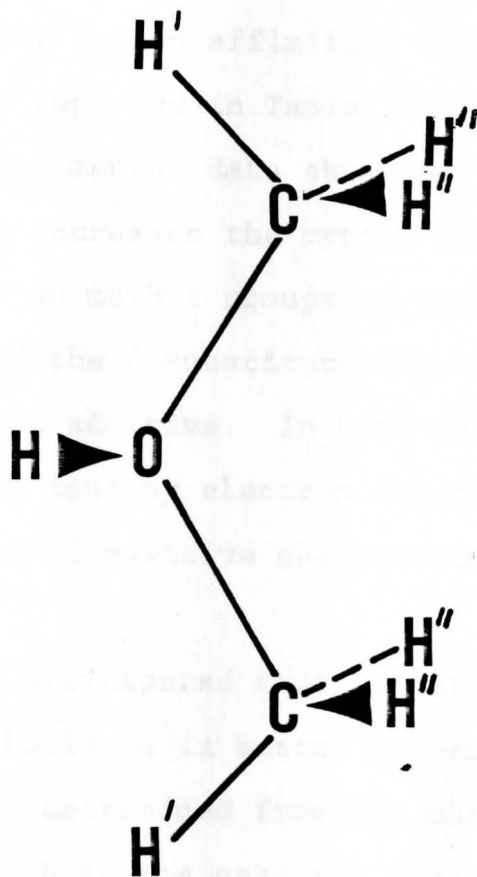


Figure 3. Equilibrium Structure of $(\text{CH}_3)_2\text{OH}^+$

Methyl Substituent Effects on Proton Affinities

The effect of methyl substitution on the proton affinities of the bases H_2O and H_2CO may be evaluated by comparing the relative proton affinities of H_2O , CH_3OH , and $(\text{CH}_3)_2\text{O}$, and of H_2CO , CH_3CHO , and $(\text{CH}_3)_2\text{CO}$. The STO-3G and 4-31G computed relative proton affinities and the experimental relative proton affinities of these two series of bases are reported in Table 12. Both theoretical and experimental data show that successive methyl substitution increases the proton affinities, and that the effect of two methyl groups on the relative proton affinities of the disubstituted bases $(\text{CH}_3)_2\text{O}$ and $(\text{CH}_3)_2\text{CO}$ is less than additive. In both series, the CH_3 groups stabilize the ions by electron donation, which results in a dispersal of positive charge primarily on the methyl hydrogens.

It would be anticipated that computed relative proton affinities should be in better agreement with experimental data when determined from the more flexible 4-31G basis set. Such is the case for the computed relative proton affinities of methyl substituted carbonyl bases. However, the computed relative proton affinities of the bases H_2O , CH_3OH , and $(\text{CH}_3)_2\text{O}$ are in better agreement with experimental data when determined from STO-3G calculations. The 4-31G calculations overestimate the

TABLE 12

Relative Proton Affinities of H_2O , CH_3OH , and
 $(\text{CH}_3)_2\text{O}$ and H_2CO , CH_3CHO , and $(\text{CH}_3)_2\text{CO}^{\text{a}}$

Base	$(-\delta\Delta E)$	$(-\delta\Delta E)$	$(-\delta\Delta H)$,
	STO-3G	4-31G	Experimental
H_2O	0.0 ^b	0.0 ^c	0.0 ^d
CH_3OH	10.0	16.7	11.9
$(\text{CH}_3)_2\text{O}$	16.9	26.4	19.8
H_2CO	0.0 ^e	0.0 ^f	0.0 ^g
CH_3CHO	15.3 (trans)	13.1 (trans)	10.4
	15.3 (cis)	12.6 (cis)	
$(\text{CH}_3)_2\text{CO}$	27.9	23.1	19.3

a) In kcal/mol.

b) Based on a computed proton affinity of 228.7 kcal/mol.

c) Based on a computed proton affinity of 183.2 kcal/mol.

d) Based on an experimental proton affinity of 170 kcal/mol, taken from ref. 2.

e) Based on a computed proton affinity of 221.3 kcal/mol.

f) Based on a computed proton affinity of 181.1 kcal/mol.

g) Based on an experimental proton affinity of 175 kcal/mol, taken from ref. 2.

stabilizing effects of the methyl groups, as the computed proton affinities of the methyl substituted bases are too high relative to H_2O . This may be due to the well-known tendency of the 4-31G basis set to flatten pyramidal angles. This is readily seen by comparing the STO-3G structures of protonated water, protonated methanol, and protonated dimethyl ether (Tables 8 and 11 and figs. 2 and 3) with the corresponding 4-31G structures given in Table 10. The 4-31G structures allow for better electron delocalization onto the methyl groups in these ions, which enhances their stabilities relative to protonated water.

From experimental data, a correlation has often been found between decreasing ionization potential and increasing proton affinity in various series of bases.³³ This correlation has been examined in this work for H_2O and its methyl substituted derivatives and for H_2CO and its methyl substituted derivatives. It is well known that the 4-31G basis set tends to overestimate ionization potentials, while the STO-3G basis set underestimates ionization potentials when compared to experimental results. Nonetheless, in the two series of methyl substituted bases, the decrease in the computed ionization potentials on successive methyl substitution parallels the decrease in experimental ionization potentials. As evident from comparing the data of Tables 12 and 13, there is a correlation between decreasing ionization potential and increasing proton

TABLE 13
 Ionization Potentials of H_2O , CH_3OH , and $(\text{CH}_3)_2\text{O}$
 and H_2CO , CH_3CHO , and $(\text{CH}_3)_2\text{CO}^{\text{a}}$

Base	STO-3G	4-31G	Experimental ^b
H_2O	10.68	13.51	12.61
CH_3OH	9.78	12.10	10.85
$(\text{CH}_3)_2\text{O}$	9.24	11.33	9.96
H_2CO	9.64	12.00	10.88
CH_3CHO	9.17	11.54	10.23
$(\text{CH}_3)_2\text{CO}$	8.76	11.16	9.70

a) In eV.

b) Experimental data taken from G. Herzberg, Molecular Spectra and Molecular Structure III. Electronic Spectra and Electronic Structure of Polyatomic Molecules, VanNostrand and Co., Inc., Princeton, N.J., (1967).

affinity in both series of bases. Such a correlation is expected, provided that the ionization potential reflects the energy required to remove an n electron from a single center which is also the site of protonation,^{17,18,34} and may be related to the common mechanism of stabilizing the resulting ions. Protonation leaves the atom at the basic site electron deficient through electron transfer to the proton, while vertical ionization of an n electron from a base leaves this same atom electron deficient through complete removal of the electron. Stabilization of the resulting ions involves electron redistribution which polarizes the electron density toward the basic site, and would therefore be influenced by the electron donating ability of substituents.¹⁸

4-31G Proton Affinities from STO-3G Geometries

From the results of the calculations on the mono- and disubstituted carbonyl bases, it has been concluded that in order to predict reliable relative proton affinities, the extended 4-31G basis set should be used. However, optimization at the 4-31G level requires the use of large amounts of computer time. In order to conserve computer time but still predict reliable relative proton affinities, an alternative to geometry optimization at the 4-31G level has been proposed.¹⁹ In the proposed method, proton affinities are computed with the 4-31G basis set using the optimized structures for the bases and ions obtained with the STO-3G basis set. To further test this approach, the relative proton affinities of the two series of bases H_2CO , CH_3CHO , and $(\text{CH}_3)_2\text{CO}$, and H_2O , CH_3OH , and $(\text{CH}_3)_2\text{O}$ have been obtained by this method, and are given in Table 14, along with the relative proton affinities computed using fully optimized 4-31G structures for the bases and ions. For H_2CO and its methyl derivatives, the proposed method predicts relative proton affinities which are in excellent agreement with the results obtained using fully optimized 4-31G structures, and with experimental data. However, for H_2O and its methyl derivatives, the agreement between the two sets of computed relative proton affinities is not as good, although the relative proton

TABLE 14

Relative Proton Affinities of Methyl
Substituted Bases Determined from 4-31G Calculations^a,

Base	From Fully Optimized 4-31G Structures	From Fully Optimized STO-3G Structures
H ₂ O	0.0 ^b	0.0 ^c
CH ₃ OH	16.7	15.1
(CH ₃) ₂ O	26.4	24.3
H ₂ CO	0.0 ^d	0.0 ^e
CH ₃ CHO	13.1	13.4
(CH ₃) ₂ CO	23.1	23.5

a) In kcal/mol.

b) Based on a computed proton affinity of 183.2 kcal/mol.

c) Based on a computed proton affinity of 181.9 kcal/mol.

d) Based on a computed proton affinity of 181.1 kcal/mol.

e) Based on a computed proton affinity of 177.7 kcal/mol.

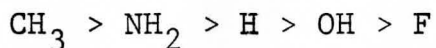
affinities obtained by the proposed method are actually in better agreement with experimental data, as evident from comparing the relative proton affinities reported in Table 14 with the experimental data from Table 12. As noted previously, there is a difference between the STO-3G and 4-31G structures of the protonated bases H_3O^+ , CH_3OH_2^+ , and $(\text{CH}_3)_2\text{OH}^+$, due to the tendency of the 4-31G basis set to flatten the pyramidal angle about the oxygen atom. This then leads to relative proton affinities which are too high for the methyl-substituted bases at the 4-31G level. It is important to note that it is the STO-3G and not the 4-31G structure of H_3O^+ which is in agreement with the structure obtained from larger basis set calculations including polarization functions.³⁵ Therefore, it appears that the proposed method of using optimized STO-3G structures for bases and ions and then carrying out single 4-31G calculations gives reasonable estimates of the relative proton affinities of related bases, and is a plausible alternative for computing reliable relative proton affinities while using a smaller amount of computer time.

The method of calculating proton affinities at the 4-31G level using optimized STO-3G geometries for the bases and ions has also been applied to determine the relative proton affinities of the series of bases ROH. As shown in Table 15, this method predicts that the order of proton

affinity of bases ROH with respect to R is



In this case, the order is the same as that obtained from the STO-3G calculations. Kollman et al¹¹ have also reported calculations on the same series of bases, and predicted the order of proton affinity to be



using a double-zeta basis set. While there is some dependence of computed proton affinities on the basis set used for the calculations, the variation in the relative proton affinities shown in Table 15 is most probably a result of the lack of geometry optimization, since Kollman did not optimize the geometry of the base, and then used the base parameters for calculations on the ions. It has already been shown that a lack of geometry optimization may lead to errors in predicting the relative proton affinities even in a series of related bases.

TABLE 15

Relative Proton Affinities of Bases ROH^a

ROH	4-31G Relative Proton Affinities from STO-3G Geometries	Relative Proton Affinities from ref. 11
R=H	0.0 ^b	0 ^c
CH ₃	15.1	11
NH ₂	-3.4	4
OH	-12.1	-6
F	-43.3	-43

a) In kcal/mol.

b) Based on a computed proton affinity of 181.9 kcal/mol.

c) Based on a computed proton affinity of 174 kcal/mol.

Conclusions

The ab initio studies of proton affinities and ion structures reported in this work support the following conclusions.

1. The order of proton affinity of the bases R_2CO with respect to R is $NH_2 > CH_3 > OH > H > F$.
2. Replacement of the hydrogen atom in RCHO by a second R group further changes the proton affinity of the base in the same direction as observed upon substitution of the first R group. Only in the case of F_2CO is the effect of two substituents more than additive.
3. Protonation of the bases R_2CO results in electron transfer to the proton, and is accompanied by a further polarization of the electron density of the base toward and within the carbonyl group. In the ions, the carbonyl oxygen remains negatively charged while the carbonyl carbon and the substituents lose electron density. The ability of the substituents to donate electrons to stabilize the positive charge is an important factor in determining the relative proton affinities of carbonyl bases.
4. There is a correlation between decreasing ionization potential and increasing proton affinity in a series of bases, provided that n-electron ionization is localized at the atom which is also the site of protonation in the base.

5. Protonation of a disubstituted carbonyl base results in a lengthening and a weakening of the carbonyl C-O bond. It may also lead to a decrease in the length of the bond between the carbonyl carbon and the substituent (the C-X bond), the magnitude of which depends upon the nature of the substituent and is essentially independent of the position of the proton.
6. Changes in the O-C-X bond angles which occur upon protonation of bases R_2CO are essentially independent of the substituent, but strongly dependent on the proton position. While the O-C-X bond angle trans to the proton decreases the O-C-X bond angle cis to the proton changes little upon protonation. The X-C-X bond angle always increases in the ion.
7. The protonation coordinates, which consist of the O-H bond length and the H-O-C bond angle, are relatively constant in the ions R_2COH^+ , suggesting that the O-H bond should be classified as a polar covalent bond.
8. The structural changes observed for the ions R_2COH^+ are similar to those observed in the ions $RCHOH^+$.
9. There is a significant basis set dependence of computed proton affinities, which are overestimated by the STO-3G basis set, but in good agreement with experimental data when computed with the 4-31G basis set.

10. The order of proton affinity of the bases ROH with respect to R is $\text{CH}_3 > \text{H} > \text{NH}_2 > \text{OH} > \text{F}$.
11. Protonation leads to a loss of electron density by the OH proton and the substituent. An inverse relationship exists between the electron density lost by the R group and the electron density lost by the H atom in the ion. The ability of the R group to donate electron density through the O-X bond is an important factor in determining the proton affinities of the bases ROH.
12. Oxygen protonation of the bases ROH leads to an increase in the bond length between the O atom and the substituent (the O-X bond). However, the change in the O-X bond length in ROH_2^+ is significantly smaller than the change in the C-O bond length in R_2COH^+ .
13. The H-O-H bond angle and the angle between the O-X bond and the HOH plane are relatively constant in the ions ROH_2^+ except in CH_3OH_2^+ and H_3O^+ where this latter angle increases to reduce the repulsion between near-by hydrogens.
14. As in the protonated carbonyls, R_2COH^+ and RCHOH^+ , the O-H bond distance in the protonated species ROH_2^+ is relatively constant.

15. The rigid monomer restriction is a severe approximation when applied to the protonated carbonyl bases R_2COH^+ , since it neglects the significant structural changes which occur in the relaxed ions. It also introduces an error into the computed relative proton affinities of the bases R_2CO , the magnitude of which depends on the nature of the substituent, and appears to be related to the change in the C-X bond length in the ions. As a result, the computed order of proton affinity of substituted carbonyl bases changes upon relaxation of this restriction.
16. The rigid monomer restriction is not as severe when applied to the protonated bases ROH_2^+ , where smaller changes in the O-X bond length occur upon protonation of the bases ROH. The computed order of proton affinity of these bases does not change when this restriction is relaxed.
17. The method of computing the relative proton affinities of related bases at the 4-31G level using the geometries of the bases and their corresponding ions optimized at the STO-3G level is a plausible alternative to full geometry optimization with the 4-31G basis set, since it provides reliable relative proton affinities using a smaller amount of computer time.

REFERENCES

- ¹L. P. Hammett, Physical Organic Chemistry, McGraw-Hill, New York, N.Y., (1970).
J. Hine, Physical Organic Chemistry, McGraw-Hill, New York, N.Y., (1962).
T. H. Lowry, and K. S. Richardson, Mechanism and Theory In Organic Chemistry, Harper and Row, New York, N.Y., (1976).
R. T. Morrison and R. N. Boyd, Organic Chemistry, Allyn and Bacon Inc., Boston, (1973).
- ²J. F. Wolf, R. H. Staley, I. Koppel, M. Taagepera, R. T. McIver, Jr., J. L. Beauchamp, and R. W. Taft, J. Amer. Chem. Soc., 99, 5417 (1977).
- ³R. W. Taft, Proton-Transfer Reactions, E. F. Caldin and F. Gold, Ed., Wiley, New York, N.Y., 1975, pp. 31-77.
- ⁴R. Yamdagni and P. Kebarle, J. Amer. Chem. Soc., 98, 1320 (1976).
- ⁵D. H. Aue, H. M. Webb, and M. T. Bowers, J. Amer. Chem. Soc., 95, 2699 (1973).
- ⁶E. M. Arnett, B. Chawla, L. Bell, M. Taagepera, W. J. Hehre, and R. W. Taft, J. Amer. Chem. Soc., 99, 5729 (1977).
- ⁷E. M. Arnett, Proton-Transfer Reactions, E. F. Caldin and V. Gold, Ed., Wiley, New York, N.Y., 1975, pp. 79-101.
- ⁸W. J. Hehre, Applications of Electronic Structure Theory, Vol. IV, H. F. Shaefer III, Ed., Plenum Press, New York, N.Y., 1977, pp. 277-331.
- ⁹F. Bernardi, I. G. Csizmadia, H. B. Schlegel, and S. Wolfe, Can. J. Chem., 53, 1144 (1975).
- ¹⁰A. C. Hopkinson and I. G. Csizmadia, Can. J. Chem., 52, 546 (1974).

¹¹A. Johansson, P. A. Kollman, J. F. Liebman, and S. Rothenberg, J. Amer. Chem. Soc., 96, 3750 (1974).

¹²L. Radom, Aust. J. Chem., 28, 1 (1975).

¹³A Pullman and P. Brochen, Chem. Phys. Letters, 34, 7 (1975).

¹⁴M. D. Newton and S. Ehrenson, J. Amer. Chem. Soc., 93, 4971 (1971).

¹⁵A. Pullman and A. M. Armbruster, Intern. J. Quantum Chem., 8S, 169 (1974); Chem Phys. Letters, 36, 558 (1975).

¹⁶J. E. Del Bene and A. Vaccaro, J. Amer. Chem. Soc., 98, 7526 (1976).

¹⁷J. E. Del Bene, J. Amer. Chem. Soc., 99, 3617 (1977).

¹⁸J. E. Del Bene, J. Amer. Chem. Soc., 100, 1673 (1978).

¹⁹J. E. Del Bene, Chem. Phys. Letters, 55, 235 (1978).

²⁰W. A. Lathan, L. A. Curtiss, W. J. Hehre, J. B. Lisle, and J. A. Pople, Prog. Phys. Org. Chem., 11, 175 (1974).

²¹J. A. Pople and D. L. Beveridge, Approximate Molecular Orbital Theory, McGraw-Hill, New York, N.Y., (1970).

J. Calais, et al, Quantum Science Methods and Structure, Plenum Press, New York, N.Y., (1976).

²²C. C. J. Roothaan, Rev. Mod. Phys., 23, 69 (1951).

²³W. J. Hehre, R. F. Stewart, and J. A. Pople, J. Chem. Phys., 51, 2257 (1969).

²⁴J. E. Del Bene, and J. A. Pople, J. Chem. Phys., 52, 4858 (1970).

- ²⁵J. E. Del Bene, J. Chem. Phys., 55, 4633 (1971).
- ²⁶J. E. Del Bene, R. Ditchfield, and J. A. Pople, J. Chem. Phys., 55, 2236 (1971).
- ²⁷R. Ditchfield, W. J. Hehre, and J. A. Pople, J. Chem. Phys., 54, 724 (1971).
- ²⁸I. Radom, W. A. Latham, W. J. Hehre, and J. A. Pople, Aust. J. Chem., 25, 1601 (1972).
- ²⁹H. Umeyama and K. Morokuma, J. Amer. Chem. Soc., 98, 4400 (1976).
- ³⁰R. S. Mulliken, J. Chem. Phys., 23, 1833 (1955).
- ³¹J. E. Del Bene, G. T. Worth, F. T. Marchese and M. E. Conrad, Theor. Chim. Acta, 36, 195 (1975).
- ³²L. J. Bellamy, The Infra-red Spectra of Complex Molecules, Chapman and Hall, London, (1975).
- L. J. Bellamy, Advances in Infrared Group Frequencies, Chapman and Hall, London, (1968).
- ³³J. L. Beauchamp, Annu. Rev. Phys. Chem., 22, 527 (1971).
- ³⁴R. H. Staley, J. E. Kleckner, and J. L. Beauchamp, J. Am. Chem. Soc., 98, 2081 (1976).
- ³⁵P. A. Kollman and C. F. Bender, Chem. Phys. Letters., 21, 271 (1973).